

Electron pair emission from W(110): Response to a spin-polarized surface stateF. Giebels,¹ H. Gollisch,¹ and R. Feder^{1,2}¹*Theoretische Festkörperphysik, Universität Duisburg-Essen, 47048 Duisburg, Germany*²*Max-Planck Institut für Mikrostrukturphysik, Weinberg 2, 06120 Halle, Germany*

(Received 16 November 2012; published 17 January 2013)

Details of a spin-polarized surface state on W(110) with a Dirac-cone-like dispersion are revealed by calculations of the spin- and layer-resolved density of states. After collisions of spin-polarized low-energy electrons, which impinge on the surface, with the surface-state electrons, correlated electron pairs are emitted, which have either parallel or antiparallel spins. Calculations of the corresponding reaction cross sections demonstrate, first, a spin-resolved mapping of the surface-state dispersion with surface-parallel momentum. Second, momentum distributions of the outgoing electron pairs with parallel and antiparallel spins allow a separation of Coulomb correlation and exchange effects.

DOI: [10.1103/PhysRevB.87.035124](https://doi.org/10.1103/PhysRevB.87.035124)

PACS number(s): 73.20.At, 71.70.Ej, 79.60.—i

I. INTRODUCTION

Due to the breaking of inversion symmetry at crystalline surfaces, spin-orbit coupling (SOC) can produce spin-polarized surface states even on nonmagnetic materials. A classical example is the *sp*-like Shockley surface state on the Au(111) surface (cf. a comprehensive theoretical and experimental investigation in Ref. 1, where ample references to previous work may be found). In short, this state is split by SOC into two with nearly parabolic dispersions $E(\vec{k}^{\parallel})$ (energy versus surface-parallel momentum), which are slightly displaced with respect to each other. Both are spin polarized in the surface plane normal to \vec{k}^{\parallel} , but with opposite spin orientation.

A completely different type of surface state (strictly speaking, a surface resonance, slightly degenerate with a bulk band) was found in photoemission experiments on the W(110) surface (cf. Refs. 2–5 and references therein). At the center $\bar{\Gamma}$ of the surface Brillouin zone (SBZ), it resides in a bulk energy-band gap at the Γ point, which originates from SOC. Going away from $\bar{\Gamma}$, it exhibits a Dirac-cone-like linear dispersion $E(\vec{k}^{\parallel})$ and is spin polarized in the surface plane normal to \vec{k}^{\parallel} , as was reported in recent spin-resolved photoemission studies.^{4,5}

This surface state on W(110) offers a good opportunity for studying the spin dependence of the electron-electron interaction in a nonmagnetic material. In the present work, we demonstrate this by a theoretical investigation of the collision of spin-polarized low-energy electrons, which impinge on the surface, with the spin-polarized surface-state electrons, leading to the emission of two correlated electrons into the vacuum. The reaction cross section for this so-called (*e*,2*e*) process (cf. Ref. 6 and very recent papers, Refs. 7–9, and ample references therein) is calculated as a function of the momentum and spin of the primary electron and of the momenta and spins of the two outgoing electrons.

As a prerequisite, we calculated the \vec{k}^{\parallel} -, layer-, and spin-resolved density of states of the W(110) surface, which show good agreement with the linear dispersion of the surface state and its spin polarization and spatial symmetry, which were revealed by recent photoemission experiments.^{4,5}

Our (*e*,2*e*) results reveal how the surface-state branches of opposite spin polarization manifest themselves in spin-

dependent energy distributions for a fixed sum energy of the two outgoing electrons. This allows a spin-resolved mapping of the surface-state dispersion relation. Angular distributions (which are equivalent to parallel momentum distributions) of the two outgoing electrons with equal energies and with antiparallel spins, which are correlated only by the Coulomb interaction, exhibit a central depletion zone (correlation hole), which is smaller than the one for electrons with parallel spins, which in turn are correlated by both Coulomb and exchange interaction.

The paper is organized as follows. In Sec. II, we outline the theoretical framework and specify the input used for its application to the W(110) surface. In Sec. III, we present and discuss results of numerical calculations of the layer- and spin-resolved density of states, and of (*e*,2*e*) energy and momentum distributions due to collisions of spin-polarized incident electrons with the spin-polarized electrons of the W(110) surface state. Section IV presents our conclusion.

II. FORMALISM AND MODEL

For our (*e*,2*e*) calculations, we employed a formalism, which has been presented in detail in earlier works (cf. Refs. 6 and 10). It may, therefore, suffice to briefly recall its key features and formulas before proceeding to specifications for the present application to the W(110) surface.

A primary electron with energy E_1 , surface-parallel momentum component \vec{k}_1^{\parallel} , and spin orientation σ_1 relative to an axis \vec{e} (i.e., spin-polarization vector $\vec{P}_1 = \sigma_1 \vec{e}$ at the electron gun) collides with a valence electron with energy E_2 , surface-parallel momentum component \vec{k}_2^{\parallel} , and spin label σ_2 , and two outgoing electrons with $(E_3, \vec{k}_3^{\parallel}, \sigma_3)$ and $(E_4, \vec{k}_4^{\parallel}, \sigma_4)$ are detected. The four one-electron states $|E_i, \vec{k}_i^{\parallel}, \sigma_i\rangle$, in the following written as $|i\rangle$, with $i = 1, 2, 3, 4$, are solutions of the Dirac equation with a complex effective potential. The primary electron state $|1\rangle$ is a low-energy electron diffraction (LEED) state and the outgoing electron states $|3\rangle$ and $|4\rangle$ are time-reversed LEED states. While these states have definite spin orientation σ_i at the source and at the two detectors, respectively, inside the solid they involve parts with σ_i and parts with $-\sigma_i$ as a consequence of spin-orbit coupling. For the valence electron state $|2\rangle$, $\sigma_2 = \pm i$, in general, only a label to

characterize two degenerate states with spin-orbit coupling. The initial two-particle state $|1,2\rangle$ is an antisymmetrized product of states $|1\rangle$ and $|2\rangle$. The final two-electron state $|3,4\rangle$ includes the Coulomb correlation between the one-electron states $|3\rangle$ and $|4\rangle$ (as described in detail in Ref. 10).

For a spin-polarized primary beam impinging on a surface system, the spin-resolved $(e,2e)$ scattering cross section (“intensity”) is then given by the golden rule form

$$I_{\sigma_3, \sigma_4}^{\sigma_1} = \frac{k_3 k_4}{k_1} \sum_{E_2, \vec{k}_2^{\parallel}, \sigma_2, n_2} | \langle 3,4 | U | 1,2 \rangle |^2 \delta, \quad (1)$$

where $k_i = \sqrt{2E_i}$ (for $i = 1, 3, 4$) and U is the screened Coulomb interaction. In the summation over the valence states $|2\rangle$, the index n_2 accounts for possible further degeneracies. Here, δ symbolizes the conservation of energy and surface-parallel momentum,

$$E_1 + E_2 = E_3 + E_4 \quad \text{and} \quad \vec{k}_1^{\parallel} + \vec{k}_2^{\parallel} = \vec{k}_3^{\parallel} + \vec{k}_4^{\parallel} + \vec{g}^{\parallel}, \quad (2)$$

where \vec{g}^{\parallel} is a surface-reciprocal lattice vector. For fixed energies and parallel momenta of the primary electron and of the two detected electrons, one thus “picks out” valence electrons with definite energy and parallel momentum.

As a prerequisite for the application to the W(110) surface, we calculated the electronic structure of the ground state by means of an *ab initio* full-potential linear augmented-plane-wave (FLAPW) method.¹¹ Using a local density approximation (LDA) for the exchange-correlation energy,¹² we applied this method to a W(110) film consisting of 11 monoatomic layers, with the first interlayer spacing reduced by 3% relative to the bulk interlayer spacing on the grounds of LEED analyses.^{13–15} We thereby obtained, in particular, a real one-electron potential, which we used to construct the complex quasiparticle potential input for calculating the $(e,2e)$ reaction cross sections and the valence electron spectral function (density of states), which is relevant for the $(e,2e)$ and the photoemission process.

The real potential was cast into the muffin-tin form, which is required by our present multiple-scattering formalism, and its LDA surface-potential barrier was replaced by one which in particular has an image-potential asymptotic behavior. The effective quasiparticle potential was then obtained by adding a spatially uniform energy-dependent complex-energy correction $V_{re} + iV_{im}$, where V_{im} is the imaginary part of the self-energy accounting for electron and hole lifetimes. Ideally, V_{re} would only be the real part of the self-energy. Since, however, our ground-state potential deviates from the ideal one, first because of the local-density approximation to the exchange-correlation functional and second because of the muffin-tin approximation, we incorporate these deviations into an effective V_{re} , which is determined such that densities of states and LEED spectra are in line with experimental data. On the grounds of photoemission data,⁴ we thus obtained for the valence electrons a spatially uniform energy-dependent V_{re} of the order of magnitude -0.1 eV. For the primary electron and the two detected electrons, which are represented by LEED states, comparison of experimental LEED spectra^{16,17} with presently calculated ones implied a constant $V_{re} = 0.8$ eV.

The imaginary part V_{im} of the self-energy was chosen as follows. For the valence electrons we used, guided by

peak widths in photoemission experimental data,^{3,4} $V_{im} = -0.025 - (|E - E_F|^2) / (|E - E_F|^2 + 64.0)$, where E is the electron energy (in eV) and E_F is the Fermi energy. For the primary electron and the two detected electrons, an appropriate form for the imaginary potential part is $V_{im} = -0.1(E + \phi)^{0.83}$, where E is the kinetic energy (relative to the vacuum level) and $\phi = 5.07$ eV is the work function of W(110). LEED spectra calculated using this V_{im} were found to agree well with experiment in Ref. 18. Further LEED calculations, which we performed in the course of the present work, yielded good agreement with earlier experimental data.^{16,17}

The surface-potential barrier is represented by a continuous form with image-potential asymptotic behavior, which is described in detail in Ref. 18. It involves two parameters: the image plane position z_1 and the matching plane position $z_2 > z_1 > 0$ above the topmost internuclear plane at $z = 0$. For the LEED-type electrons, we used it with the parameters determined by the LEED study in Ref. 18: $z_1 = 1.8$ Bohr and $z_2 = 3.6$ Bohr. For the valence electrons, we chose the barrier parameters $z_1 = 2.945$ Bohr and $z_2 = 5.890$ Bohr such that the surface resonance at the SBZ center is at 1.25 eV below the Fermi energy, in agreement with experimental data.^{3,4} Comparing the two barriers, we note that due to dynamical effects, the barrier for LEED electrons is further inward (closer to the topmost internuclear plane), which is classically plausible from the retardation of the image charge.

For the screened Coulomb interaction U in Eq. (1), we used the Thomas-Fermi approximation $U = \exp(-q_{TF}r)/r$. The value of the Thomas-Fermi wave number q_{TF} was taken as 0.2 Bohr⁻¹, in line with a result obtained by comparing calculated $(e,2e)$ energy and momentum distributions from Fe(001) with their experimental counterparts.⁷ This screening strength is significantly weaker than the one in the bulk material, since it summarily accounts for the weaker screening in the few topmost atomic layers, from which most of the electron pairs originate, and in the near-surface vacuum.

III. PAIR EMISSION RESULTS FROM W(110)

We first recall a selection rule, which is important for the $(e,2e)$ process in our present study on W(110) (cf. Ref. 19). If the reaction plane (containing the momentum vectors of the incident electron and of the two outgoing ones) is a mirror plane of the semi-infinite surface system, then only valence electron states with even reflection symmetry are allowed to contribute to the $(e,2e)$ reaction cross section. This is strictly valid in the absence of spin-orbit coupling (SOC). With SOC, the valence electron spinor generally contains both even and odd spatial parts, but its even spatial part is the most relevant one for $(e,2e)$. The odd part may contribute because, due to SOC, the incident and outgoing electron spinors also have odd parts (inside the crystal). Since these are much smaller than their even parts, $(e,2e)$ contributions involving odd valence electron parts are generally also much smaller. In the following, our coordinate system is such that z is along the (outward-directed) surface normal $[110]$ and x and y are in the surface plane along $[001]$ and $[1-1\ 0]$, respectively. Let the reaction plane be (x,z) . Due to parallel momentum conservation

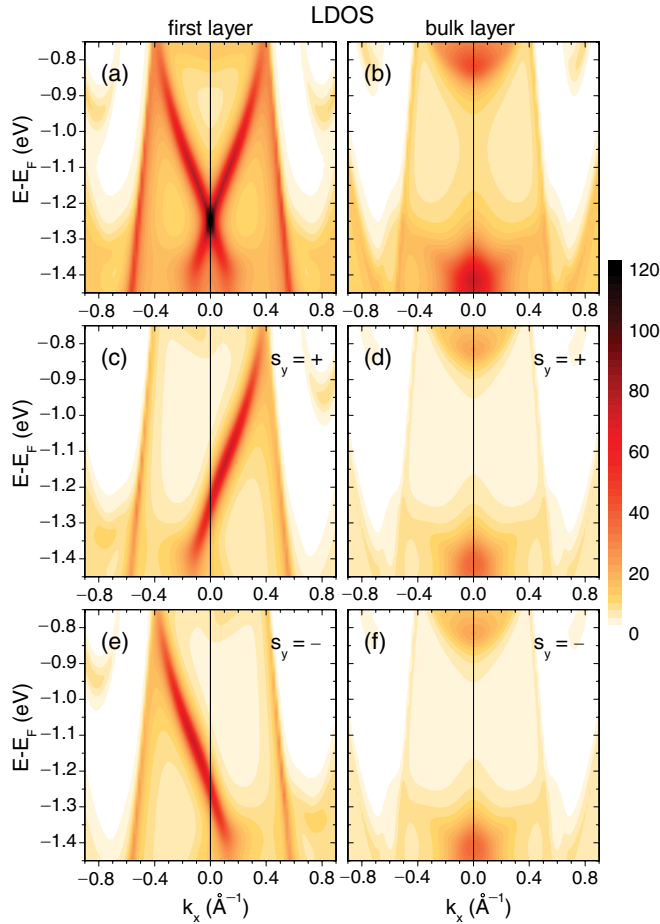


FIG. 1. (Color online) Layer-resolved valence electron densities of states (LDOS) $N_m(E, k_x; k_y = 0)$ of W(110) (with k_x in the central part of the $\bar{H}-\bar{\Gamma}-\bar{H}$ line in the surface Brillouin zone, and \bar{H} being at $k_x = 1.49 \text{ \AA}^{-1}$) of even symmetry with respect to the (x, z) plane. The coordinates x and y are in the surface plane along $[001]$ and $[1-10]$, respectively, and z is along the surface normal $[110]$. Spin-unresolved LDOS (a) N_1 for the topmost atomic layer and (b) N_b for bulk layer. N_1 and N_b resolved with spin (c), (d) in $+y$ direction and (e), (f) in $-y$ direction.

[cf. Eq. (2)], the parallel momentum of the valence electron then only has an x component.

In Fig. 1, we show the \vec{k}^{\parallel} - and layer-resolved density of states (LDOS) (alias spectral function) of even xz mirror symmetry for $\vec{k}^{\parallel} = (k_x, k_y = 0)$ along the central part of the $\bar{H}-\bar{\Gamma}-\bar{H}$ line in the surface Brillouin zone (SBZ). For $k_x = 0$, the bulk LDOS [Fig. 1(b)] exhibits, as a consequence of SOC, a gap between the peak features around -0.8 and -1.4 eV, respectively, which extends out to $k_x \neq 0$. In this gap, a surface state resides [see Fig. 1(a)], which at the center of the SBZ is at the energy -1.25 eV below E_F and disperses outward linearly up to about $\pm 0.2 \text{ \AA}^{-1}$ as a Dirac cone, in accordance with recent experimental photoemission results.⁴ The even LDOS, which is shown in Fig. 1(a) because of its relevance for $(e, 2e)$, is in fact the vastly dominant part for the surface state, whereas its odd LDOS contribution is by an order of magnitude smaller. The mainly even xz mirror symmetry of the Dirac-cone surface state, which we

thus found theoretically, was recently experimentally revealed by photoemission making use of selection rules for p - and s -polarized light.⁵ The LDOS in Figs. 1(a) and 1(b) is not spin resolved. Resolving it with respect to spin orientation along the y axis ($[1-10]$ in the surface plane) reveals that the Dirac-cone surface state consists of two parts with opposite spin polarization [Figs. 1(c) and 1(e)], whereas for the bulk, Figs. 1(d) and 1(f) are identical, i.e., no spin polarization. This spin structure of the surface state agrees perfectly with the one observed in a recent spin-resolved photoemission experiment.⁴

For a more quantitative and detailed view, we show in Figs. 2(a)–2(d) the spin- and layer-resolved even LDOS as line plots at the selected energy $E_F - 0.95$ eV. The weight of the oppositely spin-polarized surface states at $k_{2x} = \pm 0.27 \text{ \AA}^{-1}$ is strongest in the topmost atomic layer and decreases monotonously for deeper layers.

We now want to explore the electron pair emission, which results from the collisions of these spin-polarized valence state electrons with spin-polarized electrons impinging on the surface. To this end, we first choose a coplanar $(e, 2e)$ setup, with normal incidence of the primary electron and the emitted electrons in the (x, z) plane at equal polar angles $\vartheta_3 = \vartheta_4$. For fixed primary energy E_1 and constant sum energy $E_3 + E_4$ of the outgoing electrons, energy conservation [cf. Eq. (1)] then dictates a fixed valence energy E_2 . The reaction cross sections $I_{\sigma_3, \sigma_4}^{\sigma_1}$ then depend only on the energy difference $E_3 - E_4$, or, equivalently [as is easily derived from the conservation conditions given by Eq. (2)], on the valence electron parallel momentum component k_{2x} .

By choosing the primary energy $E_1 = 27$ eV and the sum energy of the two emitted electrons $E_3 + E_4 = 20.98$ eV, we select the same valence energy $E_2 = E_F - 0.95$ eV $= -6.02$ eV (with the Fermi energy $E_F = -5.07$ eV relative to the vacuum level) as for the LDOS in Figs. 2(a)–2(d). In Figs. 2(e) and 2(f), we show for this energy the spin-dependent $(e, 2e)$ intensities $I_{\sigma_3, \sigma_4}^{\sigma_1}$ [cf. Eq. (1)] as functions of the valence electron parallel momentum component k_{2x} . Consider first the primary spin σ_1 in the $+y$ direction [Fig. 2(e)], i.e., parallel to the surface-state electron spin around $k_{2x} = +0.27 \text{ \AA}^{-1}$ and antiparallel to the one around $k_{2x} = -0.27 \text{ \AA}^{-1}$. Therefore, in the former case, the intensity I_{++}^+ (with parallel spins of the two outgoing electrons) vastly dominates, whereas in the latter case, we have exclusively the intensity $I_{+-}^+ + I_{-+}^+$ (with antiparallel spins of the outgoing electrons). If the primary spin is reversed (i.e., σ_1 in the $-y$ direction), then one obtains analogous results, with all spins reversed, as can be seen in Fig. 2(f). Due to spin-orbit coupling, it is possible that an incident spin-up (spin-down) electron produces two spin-down (spin-up) emitted electrons, i.e., the intensities I_{--}^- and I_{++}^- are nonzero. They are, however, for the present geometry, vanishingly small and therefore not shown.

The manifestation of the $+y$ and $-y$ spin-polarized surface-state LDOS in pair emission spectra with parallel and antiparallel spins of the emitted electrons, which was found (in Fig. 2) for the valence state energy $E_2 = E_F - 0.95$ eV, persists over the entire energy range of the surface state, as is demonstrated in Fig. 3. Figures 3(a)–3(f) display the spin-resolved LDOS, which was shown in Fig. 1 by contour plots, for a representative selection of energies in the form of line plots. For primary

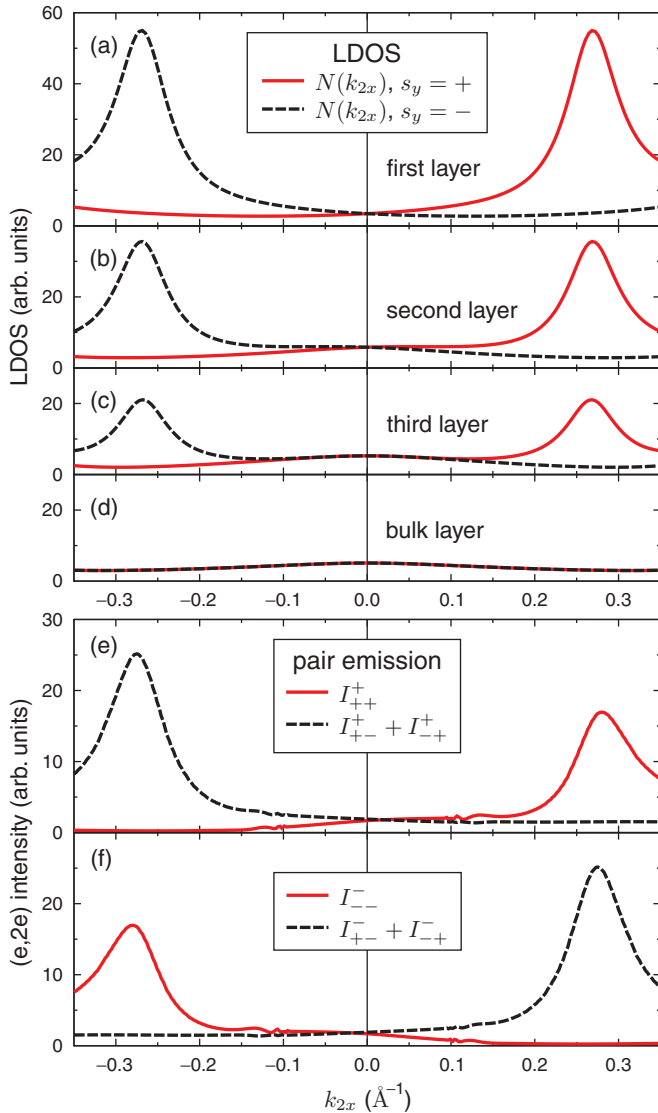


FIG. 2. (Color online) Layer- and spin-resolved valence electron density of states (LDOS) of W(110) at energy $E_2 = E_F - 0.95$ eV as a function of k_{2x} along the ΓH direction in the surface Brillouin zone for states of even symmetry with respect to the (x,z) plane [the reaction plane in our $(e,2e)$ setup]. Panels (a)–(c) show the LDOS of the three topmost layers and (d) shows the bulk layer LDOS. In panels (a)–(d), the black (dashed) lines represent the LDOS for states with spin in the $-y$ direction (in the surface plane), and the red (solid) lines represent the LDOS for spin in the $+y$ direction. Panel (e) shows spin-dependent $(e,2e)$ intensities [cf. Eq. (1)] associated with the above LDOS. The primary electron with energy 27 eV and spin $\sigma_1 = +$ in the y direction impinges normally on the surface. The two outgoing electrons with spins $\sigma_3 = \pm$ and $\sigma_4 = \pm$ propagate in the (x,z) plane with equal polar angles $\vartheta_3 = \vartheta_4 = 50^\circ$ and azimuthal angles $\varphi_3 = 0^\circ$ and $\varphi_4 = 180^\circ$, respectively. The sum of the energies of the two outgoing electrons is constant such that—by virtue of energy conservation—the energy of the valence electron is the same as in the above LDOS panels. The intensities are plotted as functions of the valence electron parallel momentum component k_{2x} , which is uniquely determined by energy and parallel momentum conservation [cf. Eq. (2)]. The black (dashed) curve relates to outgoing electrons with antiparallel spins, whereas the red (solid) curve is obtained for parallel spins. Panel (f) is analogous to (e), with all spins reversed.

spin polarization in the $+y$ direction, the corresponding pair emission spectra are shown in Figs. 3(g)–3(l). Comparing them with the adjacent LDOS panels, it is obvious that the dispersion of the $+y$ and the $-y$ polarized surface state is directly mapped by the pair emission intensities with parallel and antiparallel spins of the two emitted electrons, respectively. The fine structure in the spectra around $k_{2x} = \pm 0.1 \text{ \AA}^{-1}$ can be traced back to a surface resonance in one of the inverse LEED states, which are correlated by the Coulomb interaction to form the outgoing two-electron state. Resonances of this type are well known to occur in two-electron and electron-positron emission²⁰ and also in photoemission,²¹ for which the final state is an inverse LEED state. In the present surface-state mapping, they can be avoided by choosing a different primary energy and/or different emission angles.

The option found above to obtain electron pairs either with parallel spins or with antiparallel ones allows a disentanglement of correlation effects due to exchange and to Coulomb interaction: for antiparallel spins, there is only the Coulomb correlation, whereas for parallel spins, there are both. In the following, we shall demonstrate this disentanglement for the exchange-correlation hole in the two-electron momentum distribution. To this end, we choose the energy and surface-parallel momentum conditions [cf. Eq. (2)] such that a valence state with polarization along $+y$ is picked out at energy $E_F - 0.95$ eV and surface-parallel momentum ($k_{2x} = +0.27 \text{ \AA}^{-1}$, $k_{2y} = 0$). For the primary energy 27 eV, this is achieved, first, by choosing both outgoing electron energies as 10.49 eV and, second, by having the primary beam incident at polar angle $\vartheta_1 = 5.81^\circ$ and azimuthal angle $\varphi_1 = 180^\circ$, which implies $k_{1x} = -0.27 \text{ \AA}^{-1}$ (compensating the valence electron momentum), and observing the two equal-energy outgoing electrons at equal polar but opposite azimuthal angles, i.e., with opposite parallel momenta $\vec{k}_4^\parallel = -\vec{k}_3^\parallel$.

In Fig. 4, we show spin-resolved $(e,2e)$ momentum distributions from W(110) in the surface-parallel momentum plane $(k_x, k_y)/k := (k_{3x}, k_{3y})/k = -(k_{4x}, k_{4y})/k$ of the outgoing electrons. We first address the fully spin-resolved distributions $I_{\sigma_3\sigma_4}^{\sigma_1}(k_x, k_y)$ [cf. Eq. (1)]. For primary spin up ($\sigma_1 = +$), the intensity I_{++}^+ with parallel spins up of the two emitted electrons [Fig. 4(a)] is seen to be overall much larger than I_{+-}^+ and I_{-+}^+ [Figs. 4(b) and 4(c)] with one of the emitted electrons having spin down. Since I_{++}^+ originates mainly from a valence state with dominant spin up, whereas I_{+-}^+ and I_{-+}^+ require one of mainly spin down, this difference in magnitude is immediately plausible from the valence electron densities of states, which were shown in Fig. 2. For our chosen momentum component $k_{2x} = +0.27 \text{ \AA}^{-1}$, the spin-up LDOS in the first few layers exhibits the very pronounced surface-state peak, whereas the spin-down LDOS, which reflects bulklike states, is by far smaller. In the case of primary spin down, this entails that I_{--}^- [Fig. 4(e)] is much weaker than I_{-+}^- and I_{+-}^- [Figs. 4(f) and 4(g)], which are associated with the surface state. The intensities I_{+-}^- and I_{-+}^- , which we already mentioned to exist due to SOC, are almost everywhere extremely small and therefore not shown in Fig. 4.

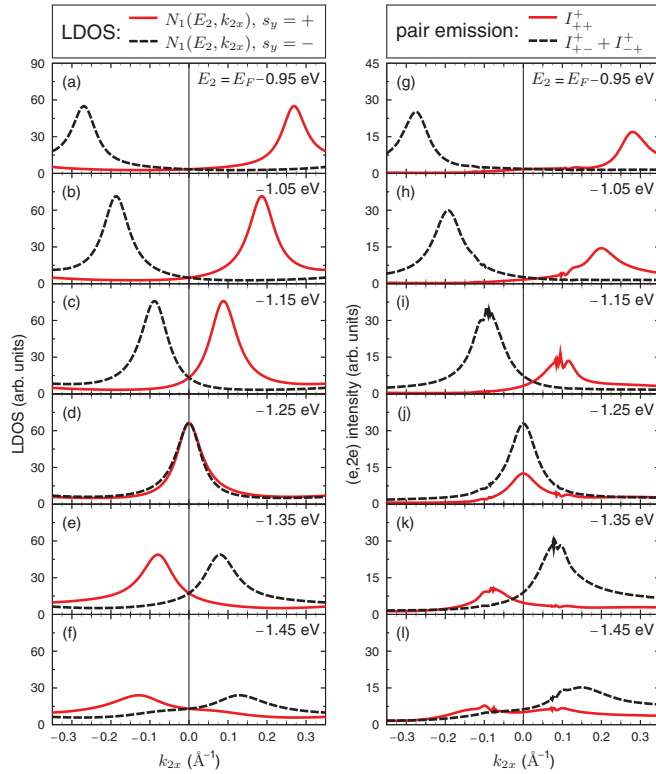


FIG. 3. (Color online) Left-hand column: Spin-resolved valence electron density of states $N_1(E_2, k_{2x})$ of the topmost atomic layer of W(110) (with k_{2x} along the $\overline{\Gamma H}$ direction in the surface Brillouin zone) for states of even symmetry with respect to the (x, z) plane [the reaction plane in our $(e, 2e)$ setup] for valence electron energy values E_2 , as indicated in the individual panels. The black (dashed) lines represent the LDOS for states with spin in the $-y$ direction (in the surface plane), and the red (solid) lines represent the LDOS for spin in the $+y$ direction. Right-hand column: Spin-dependent $(e, 2e)$ intensities [cf. Eq. (1)] from W(110) for primary electron energy 27 eV and spin in the $+y$ direction as functions of the valence electron parallel momentum k_{2x} , analogous to those shown in Fig. 2(e) and explained in its caption, except that the sum of the energies of the two outgoing electrons now assumes a series of constant values such that—by virtue of energy conservation—the energy of the valence electron (indicated in each panel) is the same as in the adjacent LDOS panel.

Next, we turn to the symmetry properties of the momentum distributions $I_{\sigma_3\sigma_4}^{\sigma_1}(k_x, k_y)$. Since the complete setup (crystal plus primary and emitted electrons) has mirror symmetry with respect to the (x, z) plane (normal to the surface), all of the momentum distributions are symmetric with respect to the k_x axis. The distributions with parallel spins of the two emitted electrons [Figs. 4(a) and 4(e)] are, furthermore, symmetric with respect to the k_y axis. This is due to the fact that changing (k_x, k_y) into $(-k_x, -k_y)$ leaves the physical situation unchanged. As regards the antiparallel-spin electrons, changing (k_x, k_y) into $(-k_x, -k_y)$ interchanges their spins. Consequently, the mirror operation at the k_y axis interchanges, for each primary spin $\sigma_1 = \pm$, the distributions $I_{+-}^{\sigma_1}$ and $I_{-+}^{\sigma_1}$, i.e., Figs. 4(b) and 4(c) for $\sigma_1 = +$ and Figs. 4(f) and 4(g) for $\sigma_1 = -$.

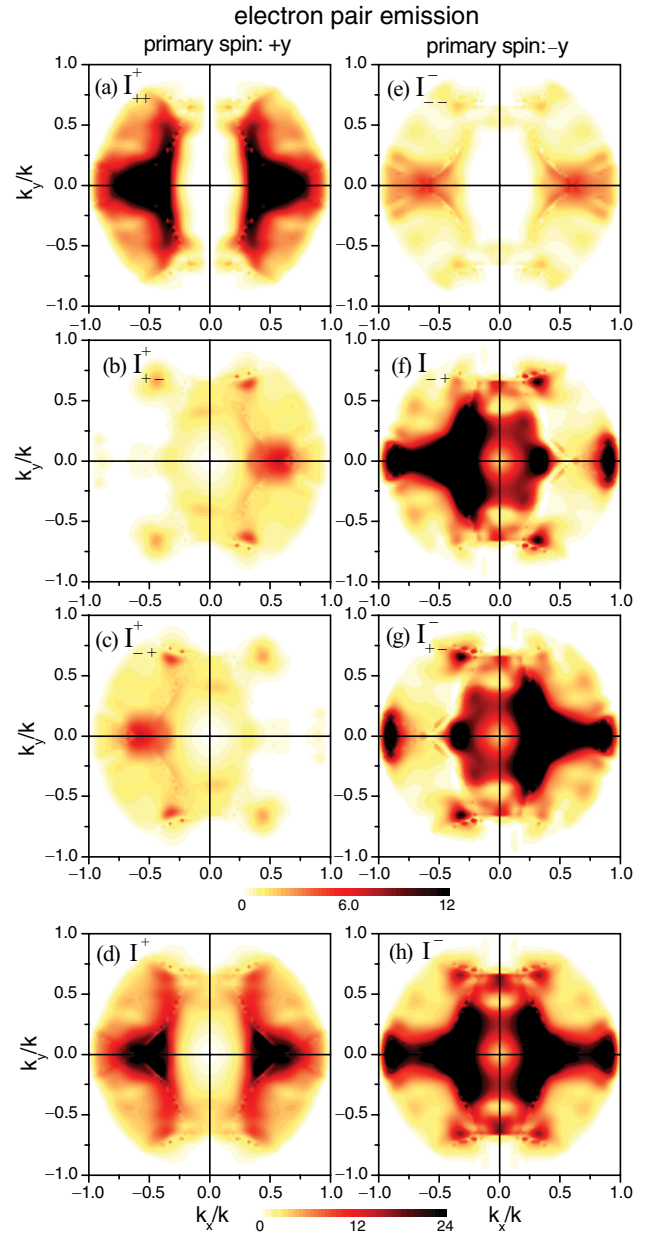


FIG. 4. (Color online) Spin-resolved $(e, 2e)$ momentum distributions [cf. Eqs. (1) and (3)] from W(110) in the surface-parallel momentum plane $(k_x, k_y)/k$. Primary electrons with energy 27 eV are incident at polar angle $\vartheta_1 = 5.81^\circ$ and azimuthal angle $\varphi_1 = 180^\circ$, i.e., in the (x, z) plane with surface-parallel momentum component $k_{1x} = -0.27 \text{ \AA}^{-1}$. The two electrons are emitted at polar angle ϑ , and azimuthal angles φ and $\varphi + \pi$, respectively. They have equal energies $E = 10.49 \text{ eV}$ and surface-parallel momenta $(k_x, k_y) = \sqrt{2E} \sin \vartheta (\cos \varphi, \sin \varphi)$ and $(-k_x, -k_y)$. The relevant valence electron thus has energy -0.95 eV relative to the Fermi energy and parallel momentum components $k_{2x} = 0.27 \text{ \AA}^{-1}$ and $k_{2y} = 0 \text{ \AA}^{-1}$. As can be seen from the LDOS in Fig. 3(a), it is a surface-state electron with spin polarization in the $+y$ direction. Panels (a)–(c) and (e)–(g) show the fully spin-resolved intensities $I_{\sigma_3\sigma_4}^{\sigma_1}(k_x, k_y)$ [cf. Eq. (1)] with spin quantization along the y axis and values \pm of the primary electron spin σ_1 and the spins σ_3 and σ_4 of the emitted electrons, as indicated in the individual panels. The total intensities I^+ and I^- [cf. Eq. (3)] for primary spin up and down are presented in panels (d) and (h), respectively.

The most important conclusion is reached by comparing the momentum distributions for parallel spins of the outgoing electrons [Figs. 4(a) and 4(e)] with those for antiparallel spins [Figs. 4(b) and 4(c) and Figs. 4(f) and 4(g)]. Going outward from the center, all distributions exhibit a region of small intensity. This depletion zone is seen to be much more pronounced for parallel spins than for antiparallel ones. Since outgoing electrons with parallel spins are subject to exchange and Coulomb interaction, whereas those with antiparallel spins are correlated only by the Coulomb interaction, the central depletion zones in the antiparallel-spin distributions I_{+-}^{\pm} and I_{-+}^{\pm} can be viewed as a Coulomb correlation hole and those in the parallel-spin ones I_{++}^+ and I_{--}^- as an exchange plus Coulomb correlation hole. Our momentum distributions thus imply that the latter hole is much larger than the former.

With regard to an experimental realization, we note that—spin resolution of the outgoing electrons being presently not feasible—the observable quantities are, for primary spin $\sigma_1 = \pm$, the sums I^{\pm} over the spins of the emitted electrons,

$$I^+ := I_{++}^+ + I_{+-}^+ + I_{-+}^+ + I_{--}^+, \quad (3a)$$

$$I^- := I_{--}^- + I_{-+}^- + I_{+-}^- + I_{++}^-, \quad (3b)$$

i.e., essentially the sums over Figs. 4(a)–4(c) and 4(e)–4(g), respectively. As is evident from Fig. 4, the I^+ distribution [Fig. 4(d)] still exhibits the main features of the resolved parallel-spin intensity I_{++}^+ [Fig. 4(a)], and I^- [Fig. 4(h)] exhibits those of the sum of the antiparallel-spin intensities I_{-+}^- [Fig. 4(f)] and I_{+-}^- [Fig. 4(g)]. A separation of Coulomb and exchange correlation appears therefore experimentally possible.

IV. CONCLUSION

Our calculation of the electronic structure of the W(110) surface confirmed the experimentally observed⁴ spin polarization and almost linear dispersion of the two branches of a surface state with energy inside a SOC-induced pseudogap of the surface-projected bulk band structure.

Our main aim was to explore how this surface state manifests itself in electron-induced two-electron emission and how it offers an opportunity for separating exchange and Coulomb correlation between the two outgoing electrons.

By virtue of the conservation of energy and surface-parallel momentum in the $(e,2e)$ process, a suitable choice of the geometry and of the energies of the primary and the emitted electrons makes it possible to select surface-state electrons with a well-defined energy and parallel momentum as collision partners. Calculating the spin-dependent $(e,2e)$ intensity—for a spin-polarized primary electron colliding with a spin-polarized surface-state electron—as a function of the valence electron energy and momentum, we demonstrated how $(e,2e)$ can be used for a spin-resolved mapping of the dispersion of the two oppositely polarized surface-state branches. For a given spin of the incident electron, the surface-state branch with the same (opposite) spin leads essentially to parallel (antiparallel) spins of the two outgoing electrons.

Selecting a valence electron with fixed energy and momentum on the spin-up branch, we calculated the intensities resolved with respect to the spins of the primary and of the two emitted electrons as functions of the parallel momenta of the latter. For parallel spins of the emitted electrons, these momentum distributions exhibit, due to exchange and Coulomb correlation, a sizable central depletion zone (exchange-correlation hole). In the case of antiparallel spins, in which there is only Coulomb correlation, the depletion zone (correlation hole) is much smaller.

For primary spin up, i.e., parallel to the surface-state spin, the momentum distribution I_{++}^+ (with parallel spins of the outgoing electrons) is by far stronger than the ones with antiparallel spins of the outgoing electrons, whereas for primary spin down, I_{-+}^- and I_{+-}^- (with antiparallel spins of the outgoing electrons) are dominant. The experimentally observable sums of the momentum distributions for each primary spin over the spins of the two emitted electrons therefore still exhibit the main features of the resolved parallel-spin intensities I_{++}^+ and antiparallel-spin intensities $I_{-+}^- + I_{+-}^-$, in particular the exchange hole is much larger than the Coulomb correlation hole. A separation of Coulomb and exchange correlation appears therefore experimentally possible.

ACKNOWLEDGMENT

It is our pleasure to acknowledge lively and fruitful discussions with J. Kirschner.

¹J. Henk, M. Hoesch, J. Osterwalder, A. Ernst, and P. Bruno, *J. Phys.: Condens. Matter* **16**, 7581 (2004).

²R. H. Gaylord and S. D. Kevan, *Phys. Rev. B* **36**, 9337 (1987).

³J. Feydt, A. Elbe, H. Engelhard, G. Meister, Ch. Jung, and A. Goldmann, *Phys. Rev. B* **58**, 14007 (1998).

⁴K. Miyamoto, A. Kimura, K. Kuroda, T. Okuda, K. Shimada, H. Namatame, M. Taniguchi, and M. Donath, *Phys. Rev. Lett.* **108**, 066808 (2012).

⁵K. Miyamoto, A. Kimura, T. Okuda, K. Shimada, H. Iwasawa, H. Hayashi, H. Namatame, M. Taniguchi, and M. Donath, *Phys. Rev. B* **86**, 161411 (2012).

⁶R. Feder and H. Gollisch, *Solid State Photoemission and Related Methods*, edited by W. Schattke and M. A. Van Hove (Wiley-VCH, Weinheim, 2003), Chap. 9.

⁷F. Giebels, H. Gollisch, R. Feder, F. O. Schumann, C. Winkler, and J. Kirschner, *Phys. Rev. B* **84**, 165421 (2011).

⁸S. Samarin, O. M. Artamonov, V. N. Petrov, M. Kostylev, L. Pravica, A. Baraban, and J. F. Williams, *Phys. Rev. B* **84**, 184433 (2011).

⁹Z. Wei, F. O. Schumann, R. S. Dhaka, and J. Kirschner, *Phys. Rev. B* **85**, 195120 (2012).

¹⁰H. Gollisch, N.v. Schwartzberg, and R. Feder, *Phys. Rev. B* **74**, 075407 (2006).

¹¹See www.flapw.de (unpublished).

¹²S. H. Vosko, L. Wilk, and M. Nusair, *Can. J. Phys.* **58**, 1200 (1980).

¹³M. Arnold, G. Hupfauer, P. Bayer, L. Hammer, K. Heinz, B. Kohler, and M. Scheffler, *Surf. Sci.* **382**, 288 (1997).

¹⁴G. Teeter, J. L. Erskine, F. Shi, and M. A. Van Hove, *Phys. Rev. B* **60**, 1975 (1999).

- ¹⁵D. Venus, S. Cool, and M. Plihal, *Surf. Sci.* **446**, 199 (2000).
- ¹⁶H. J. Herlt, R. Feder, G. Meister, and E. G. Bauer, *Solid State Commun.* **38**, 973 (1981).
- ¹⁷E. G. Bauer (private communication).
- ¹⁸S. N. Samarin, J. F. Williams, A. D. Sergeant, O. M. Artamonov, H. Gollisch, and R. Feder, *Phys. Rev. B* **76**, 125402 (2007).
- ¹⁹R. Feder and H. Gollisch, *Solid State Commun.* **119**, 625 (2001).
- ²⁰F. Giebels, H. Gollisch, and R. Feder, *J. Phys.: Condens. Matter* **21**, 355002 (2009).
- ²¹A. Winkelmann, M. Ellguth, C. Tusche, A. A. Unal, J. Henk, and J. Kirschner, *Phys. Rev. B* **86**, 085427 (2012).